

Study of the conversion decays of omega meson into π^0 meson and e^+e^- pair with the CMD-3 detector

Anastasiya KUZMENKO^{*†}

Budker Institute of Nuclear Physics, Novosibirsk

Novosibirsk State University, Novosibirsk

E-mail: anastasiya.e.kuzmenko@gmail.com

The conversion decay $\omega \rightarrow \pi^0 e^+ e^-$ was studied in the center-of-mass energy range 760 – 840 MeV using about 8 pb^{-1} of data collected with the CMD-3 detector at the VEPP-2000 e^+e^- collider in Novosibirsk. The visible cross section of the process $\omega \rightarrow \pi^0 e^+ e^-$ was measured. The current status of the analysis is presented.

XXVII International Symposium on Lepton Photon Interactions at High Energies

17-22 August 2015

Ljubljana, Slovenia

^{*}Speaker.

[†]on behalf of the CMD-3 and VEPP-2000 collaborations

Introduction The interest in the decay $\omega \rightarrow \pi^0 e^+ e^-$ is related to the transition formfactors of the ω meson that can be measured in this decay [1]. The precise value of the decay branching ratio can be useful for interpretation of experiments on quark-gluon plasma. This analysis is based on 10 pb^{-1} of data, which were collected in the center-of-mass energy range 760 – 840 MeV with the CMD-3 detector. This data sample is three times larger than previously used at the former CMD-2.

The general purpose detector CMD-3 has been described in detail elsewhere [2]. The tracking system consists of the cylindrical drift chamber (DC) and double-layer multiwire proportional Z-chamber, both also used for the trigger. The tracking system is placed inside a thin superconducting solenoid with 1.3 T field. The barrel LXe with a thickness $5.4 X_0$ and CsI crystal with a thickness of $8.1 X_0$ electromagnetic calorimeters are placed outside the solenoid. The endcap calorimeter is made of BGO scintillation crystals with a thickness of $13.4 X_0$.

Data analysis The decay $\omega \rightarrow \pi^0 e^+ e^-$ has been studied using the π^0 dominant decay mode $\pi^0 \rightarrow \gamma\gamma$. It corresponds to a final state with two opposite charge particles and two photons. One of the significant resonant backgrounds comes from the $\omega \rightarrow \pi^+ \pi^- \pi^0$ decay which has the same topology of the final state and more than three orders of magnitude larger probability. Another source of resonant background is the $\omega \rightarrow \pi^0 \gamma$ decay followed by the Dalitz decay of the π^0 or γ -quantum conversion in the material in front of the drift chamber. The non-resonant background includes contributions from the following QED processes with the same final state topology: $e^+ e^- \rightarrow e^+ e^- \gamma\gamma$, $e^+ e^- \rightarrow 3\gamma$ followed by γ -quantum conversions, $e^+ e^- \rightarrow e^+ e^- \gamma$ with one background photon as well as two-quantum annihilation followed by a γ -quantum conversion and one background photon in calorimeters.

For the selection of events of the process under study, we used 25 criteria.

To suppress events from the decay $\omega \rightarrow \pi^+ \pi^- \pi^0$ we use the following parameters: opening angle between tracks ($\Delta\psi < 1$) and recoil mass of photon pairs. Recoil mass of photon pairs, where it is understood that they originated from the π^0 decay $M_{\text{rec}}^2 = (2 \cdot E_{\text{beam}})^2 - 4E_{\text{beam}}E_{\pi^0} + m_{\pi^0}^2$, where $E_{\pi^0} = E_{\gamma,1} + E_{\gamma,2}$, and $E_{\gamma,i}$ - the energy of the photon "i" in calorimeter. The recoil mass of photon pairs is shown in Figure 1. The black line in Figure 1 presents the selection cut.

The total momentum of the tracks $p = |\vec{P}_1 + \vec{P}_2|$ does not considerably differ from the photon momentum p_γ in the $\omega \rightarrow \pi^0 \gamma$ decay at a given energy $|p - p_\gamma| < 35 \text{ MeV}/c$ to suppress $\omega \rightarrow \pi^+ \pi^- \pi^0$ events as well as $\omega \rightarrow \pi^0 \gamma$ events followed by the Dalitz decay of π^0 . This condition is illustrated with horizontal lines in Figure 2. Other red lines in Figure 2 are used for selection.

Also, we required that the invariant mass of the electron-positron pair and the most energetic photon $M_{\text{inv}}(e^+ e^- \gamma_1)$ is less than $1.85 \cdot E_{\text{beam}}$ to suppress $e^+ e^- \rightarrow \gamma\gamma$ events followed by the conversion of the γ .

Separation of $\pi^0 e^+ e^-$ and $\pi^0 \gamma$ (with conversion γ on the detector material) The only difference between the $\pi^0 e^+ e^-$ and $\pi^0 \gamma$ with γ conversion on detector material is that the vertex of tracks is shifted from the beam by 1.7-2 cm (vacuum tube) in the transverse plane. To analyze these events we use $\gamma\gamma$ events, where one of γ converts on material. For separation we use a neural network with input parameters:

- the angle between the tracks;
- the total momentum normalized to beam energy;

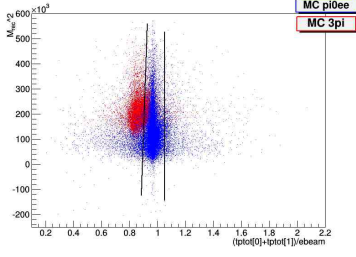


Figure 1: The recoil mass of photon pair vs the total energy of electron-positron pair, normalized to the beam energy for MC simulation of $\pi^0 e^+ e^-$ (blue dots) and $\pi^+ \pi^- \pi^0$ (red dots). The black line shows the selection cut.

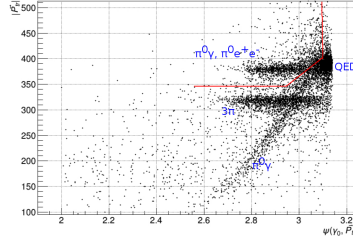


Figure 2: The total momentum of charged particles (P_{tr}) vs angle between the most energetic photon and \vec{P}_{tr} . The red lines presents the selection cuts.

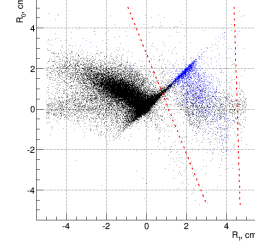


Figure 3: The distance from the beam point to the first cross-point vs distance to the second cross-point is shown for MC simulation of $\pi^0 e^+ e^-$ (black dots) and $\gamma\gamma$ with photon conversion on material (blue dots). Red lines present the alternative selection cut.

- the track momentum normalized to beam energy;
- The distance from the vertex to the center of the beam. The sign of the distance is "+" in case of the angle between the beam point direction to a cross-point and average momentum of tracks is sharp and "-" otherwise. In the transverse plane circles from tracks have two cross-points: the first one is the vertex and the second is additional. These parameters are shown in Figure 3.

Output parameter of the neural network determines the event type (signal ($\pi^0 e^+ e^-$) or background (conversion γ on the detector material)). Using this option to separate the events we got the following efficiency of suppression: for $\pi^0 \gamma$ – 84 % (for $\gamma\gamma$ – 90 %), while we lose 2 % of signal events.

Results The detection efficiency $\epsilon_{dec}^{\pi^0 e^+ e^-} = 22\%$ was determined using Monte-Carlo simulation based on the GEANT4 [3]. The number of signal and background events has been obtained from a fit of the $\gamma\gamma$ invariant mass distribution at each energy point. The signal was described by a logarithmic Gaussian, the shape of background was fixed by approximation of the $\gamma\gamma$ invariant mass at $\sqrt{s} = 660$ MeV energy point. The shape of signal curve was fixed from the fit of all experimental data in the energy range 760 – 820 MeV, so varying parameters at each energy point were the number of signal and background events. These values were used to determine the visible cross section of signal (see Figure 4, by the formula: $\sigma_{vis} = \frac{N_{sig,i}}{L_i(1+\delta_i) \cdot \epsilon_{dec} B(\pi^0 \rightarrow \gamma\gamma)}$) and background events (see Figure 5, by the formula: $\sigma_{vis\ bg} = \frac{N_{bg,i}}{L_i}$).

The current value of $Br(\omega \rightarrow \pi^0 e^+ e^-)$ (the trigger efficiency, the efficiency of reconstruction of close tracks and the contributions of $\omega \rightarrow \pi^+ \pi^- \pi^0$, $\omega \rightarrow \pi^0 \gamma$ were not taken into account) and the most important results from other experiments are presented in the Table 1.

The study of the trigger efficiency, test of the method of $\pi^0 \gamma / \pi^0 e^+ e^-$ - separation using QED events and analysis of systematics are included in the plans for the future. We also plan to process

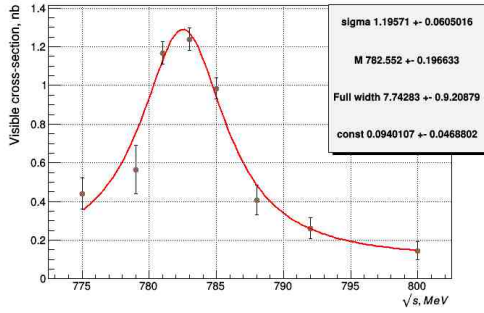


Figure 4: Visible cross section of the signal process is fitted with a Breit-Wigner distribution.

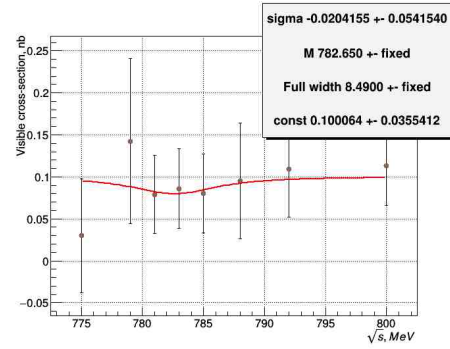


Figure 5: Visible cross section of the background events is fitted with a Breit-Wigner distribution.

| Experiment | $\text{Br}(\omega \rightarrow \pi^0 e^+ e^-)$ | events | data, pb^{-1} |
|-----------------------|--------------------------------------------------|--------|------------------------|
| ND [4] | $(5.9 \pm 1.9) \cdot 10^{-4}$ | 43 | |
| CMD-2 [5] | $(8.19 \pm 0.71 \pm 0.62) \cdot 10^{-4}$ | 230 | 3.3 |
| SND [6] | $(7.61 \pm 0.53 \pm 0.64) \cdot 10^{-4}$ | 613 | 9.8 |
| CMD-3 (preliminarily) | $(7.15 \pm 0.38) \cdot 10^{-4}$ (<i>stat.</i>) | 1228 | 8 |

Table 1: Results from current and other experiments.

all the collected data sample in the center-of-mass energy range 760 – 840 MeV with the CMD-3 detector and measurement of the transition formfactor of the ω meson.

Acknowledgment The author is grateful to V.F.Kazanin, D.N.Grigoriev, S.I.Eidelman and D.Liventsev for fruitful and useful discussions. This work is supported in part by the RFBR grants 14-02-31275 mol_a, 13-02-01134 a.

References

- [1] L. Landsberg, Phys. Rep. 128, 301 (1985).
- [2] B.I. Khazin *et al.* (CMD-3 Collaboration), Nucl. Phys. B Proc. Suppl. 181-182, 376 (2008).
- [3] S. Agostinelli *et al.* (GEANT4 Collaboration), Nucl. Instr. and Meth. A 506, 250 (2003).
- [4] S.I. Dolinsky *et al.*, Sov. J. Nucl. Phys. 277-279, 48 (1988).
- [5] R.R. Akhmetshin *et al.* (CMD-2 Collaboration), Phys. Lett. B613 29-38 (2005).
- [6] M.N. Achasov *et al.* (SND Collaboration), J. Exp. Theor. Phys. 61-68 107 (2008).